

Thermal dependence of the strain response of optical fibre Bragg gratings

Martin J. O'Dwyer*, Chen-Chun Ye, Stephen W. James and Ralph P. Tatam.

Optical Sensors Group

Centre for Photonics and Optical Engineering

School of Engineering

Cranfield University

Bedfordshire

MK43 0AL

UK

E-mail: r.p.tatam@cranfield.ac.uk

Tel. 01234 754630

Fax. 01234 752452

*presently with the Optics and Applications group in the Department of Physics and Astronomy the
University of Glasgow, Glasgow, G12 8QQ.

Abstract

The temperature dependence of the strain sensitivity of fibre Bragg gratings written into a number of different fibre types was investigated. It was found that the strain response changed on average by $0.21 \pm 0.03 \text{ fm } \mu\text{m}^{-1} \text{ } ^\circ\text{C}^{-1}$ over a range of temperatures between 100-400°C. These results were in agreement with predictions based on material parameters.

Index Terms--Bragg gratings, strain response, temperature dependence.

Introduction

One of the most significant developments in the field of optical engineering over the last two decades has been the emergence of the fibre Bragg grating (FBG), which has found major applications in telecommunications and sensor systems [1].

FBGs are formed by modulating the refractive index of the core of an optical fibre. This modulation can be achieved by exposing the fibre to a UV interference pattern [2]. The presence of the modulation, of period of order $0.5 \mu\text{m}$, results in the coupling of the forward propagating mode of the fibre to a backward propagating mode at a wavelength that satisfies the Bragg condition,

$$\lambda_B = 2n_{eff}\Lambda \quad (1)$$

Where λ_B is the Bragg wavelength, n_{eff} is the effective index of the propagating mode and Λ is the period of the refractive index modulation. A change in the period of the modulation or in the effective index of the propagating mode in response to the local environment thus gives rise to a change in the Bragg wavelength. The determination of the wavelength change is then the basis of operation of FBG sensors. The primary measurands for FBG sensors are temperature and strain.

The sensitivity of the Bragg wavelength to temperature arises from the change in period associated with the thermal expansion of the fibre, coupled with a change in the refractive index arising from the thermo-optic effect. The strain sensitivity of the Bragg wavelength arises from the change in period of the fibre, coupled with a change in the refractive index arising from the strain-optic effects. Recent studies have shown that the response to temperature exhibits a small non-linearity [3].

Some industrial and aerospace applications require sensors to operate at elevated temperatures for extended periods of time. If the strain sensitivity of FBG sensors exhibits a temperature dependence, then operation of this sensor type could be problematic if it were to be operated at a temperature that is significantly different

from that at which it was calibrated. A thermal dependence of the strain sensitivity of a FBG would result from the temperature dependence of the materials' parameters of silica glass. Previous research [4] has shown that the stress-optic coefficient of vitreous silica demonstrates a negligible temperature dependence. However, Morey *et al* [5] measured a 5 % decrease in the slope of the stress response for Germanium doped silica fibre at 650°C. A change of 8 % had been expected, based on Young's modulus data. This discrepancy was attributed to a change in the stress-optic coefficient, which they suggest represents approximately 22 % of the Bragg wavelength shift with load. A more detailed examination of the temperature dependence of the strain response of FBGs written into a number of different fibre types is presented here.

The positive thermal expansion coefficient in glasses results in a decrease in both the density and the refractive index with increasing temperature. However, the electron polarizability increases and produces an increase in the refractive index [6][7]. The electron polarizability dominates in silicate glasses, but the magnitude of its temperature sensitivity can vary by a factor of ten depending on the composition of the glass. Another possible factor affecting the refractive index is the differential expansion of the core and cladding due to their slightly different compositions. This effect could influence any changes in the fibre's density and in the electron polarizability. The fibre's composition will also affect its mechanical properties [8].

The strain sensitivity of the Bragg wavelength is generally assumed to be independent of temperature. However, it is known that the material parameters that determine the strain sensitivity, the strain optic coefficients and Poisson ratio, are themselves temperature dependent [7-9]. This paper aims to investigate the effect of the thermal sensitivity of these parameters upon the strain sensitivity of FBG sensors.

THEORY

Barlow and Payne [9] demonstrated that the stress-optic coefficient of optical fibre decreases with increasing temperature. Assuming an equivalent effect in the strain-optic coefficient it might be expected that the strain sensitivity of a FBG would increase at elevated temperatures. A theoretical analysis of the temperature effect has been performed to estimate the magnitude of the change in the strain response of a typical FBG. The dependence of the Bragg wavelength upon strain and temperatures changes is given by [10]:

$$\lambda(T, \varepsilon) = \lambda_B \left(1 + \varepsilon - \frac{1}{2} n_0^2(T) [p_{12}(T)\varepsilon + (p_{11}(T) + p_{12}(T))\nu(T)\varepsilon] + \xi T \right) \quad (2)$$

Where n_o is the unperturbed fibre refractive index, ν is Poisson's ratio, p_{12} and p_{11} are Pockels strain optic coefficients, ε is the axial strain, T is the temperature, ξ is a thermal coefficient, including thermo-optic and thermal expansion contributions. λ_B is the initial Bragg wavelength such that equation 2 describes the modified Bragg wavelength resulting from applied strain and temperature changes. Using equation 2, the axial strain sensitivity may be determined to be

$$\frac{\Delta\lambda(T)}{\Delta\varepsilon} = \lambda_B \left(1 - \frac{1}{2} n_0^2(T) [\nu(T)p_{11}(T) + p_{12}(T)[\nu(T) + 1]] \right) \quad (3)$$

The thermal dependence of the FBG strain sensitivity arises from the temperature sensitivity of the strain optic coefficients and of Poisson's ratio. Using the previously reported temperature sensitivity of these parameters, in conjunction with well established values for the material parameters, Equation 3 was used to simulate the effects of temperature on the strain response. The following parameters were used to this end: ν (Poisson's ratio) = 0.25 and $d\nu/dT \cong 2.5 \times 10^{-4} \% \text{ } ^\circ\text{C}^{-1}$ [8], $\lambda_B = 850 \text{ nm}$ and $d\lambda_B/dT = 7 \times 10^{-12} \text{ m } ^\circ\text{C}^{-1}$, $n_{eff} = 1.5$ [7], dn/dT (for silica glass) = $10.8 \times 10^{-6} \text{ } ^\circ\text{C}^{-1}$ [7], $p_{12} = 0.252$ and $p_{11} = 0.133$ [11] and $dp_i/dT = -0.134 \times 10^{-3} \text{ } ^\circ\text{C}^{-1}$ (predicted from [9]).

Figure 1 shows the temperature induced change in the strain response of an FBG with a Bragg wavelength of 850 nm calculated using the parameters given above. The gradient of this graph leads to is predicted value of the temperature dependence of the strain sensitivity to be $0.2 \text{ fm } \mu\epsilon^{-1} \text{ } ^\circ\text{C}^{-1}$.

EXPERIMENT

The experimental configuration is shown schematically in figure 2. The output from a fibre pigtailed superluminescent diode, SLD, with a central wavelength of 840 nm, a bandwidth of approximately 20nm, and a fibre coupled power of 0.5 mW, was used to illuminate the FBGs via a directional coupler. The reflected Bragg wavelengths were monitored using a tuneable filter based upon a scanning fibre Fabry-Perot (FFP) interferometer[12], manufactured by Micron Optics, with an FSR measured to be $2.3 \pm 0.7 \times 10^4 \text{ GHz}$, which is approximately equivalent to 47 nm at a centre wavelength of 830nm. The finesse was 220. The transmission of the FFP was monitored using an avalanche photodiode, APD (C5460-01, Hamamatsu Photonics). A voltage ramp was applied to the scanning FFP, and the spectrum was determined by monitoring the output from the APD in conjunction with the voltage applied to the FFP, which was calibrated such that it allowed the instantaneous resonant wavelength of the FFP to be determined.

The tensile load was applied to the FBG by anchoring it between a fixed block and the moveable platform of a translation stage, initially separated by $185 \pm 0.5 \text{ mm}$. The moveable platform was subsequently displaced by applying a voltage to an internal PZT stack. The fibre, stripped of its polyacrylate buffer jacket, was attached to the anchoring points using a cyanoacrylate strain gauge adhesive. The experimental configuration was constructed such that a tube furnace was positioned between the fibre fixing points. The FBG was located at the central region of the tube furnace, in which the temperature profile varied by $\pm 5 \text{ } ^\circ\text{C}$ along its axis over the central 4 cm of the furnace. The furnace could operate between ambient temperature

and 900°C. The oven used a PID circuit to maintain the desired temperature with an accuracy and stability of ± 1 °C.

The FBGs were fabricated in hydrogen loaded optical fibre using a UV holographic technique [13]. The fibres used are listed in Table 1. The FBGs, each of length 5mm, had bandwidths in the range 0.2-0.4 nm, and reflectivities of 30 % - 80 %. Since the concentrations and types of dopants utilized during fibre fabrication will vary between manufacturers, a number of different fibres were tested, each from a different manufacturer.

Care was taken to eliminate as many possible influences upon the characterisation of the FBG strain sensitivity. Following FBG fabrication, the fibre was maintained at room temperature and pressure for a period in excess of two weeks, allowing the hydrogen to diffuse out of the fibres [14]. Tests have shown that, under normal conditions, the refractive index modulation of FBGs fabricated in hydrogen loaded fibre decreases by ~ 15 % in the initial few weeks following FBG fabrication, corresponding to a decrease in reflectance of ~ 9 % over the first 14 days. This change is not observed in FBGs fabricated in optical fibres that were not hydrogen loaded [15].

The FBGs were then annealed at a temperature of 500 °C for seven hours. This temperature was chosen because it lies at the beginning of the transition range for silica glass, and it is likely that the fibre will behave inelastically above it. Consequently, the strain response of the FBGs will prove non-linear in the transition range and above. In fact, FBGs have been shown to exhibit hysteresis in the transition range [5], and so 500 °C may be considered to be the upper temperature limit for the operation of FBGs. All fibres were annealed under the same conditions, as previous studies have shown that the response to annealing is largely independent of fibre composition [15].

Annealing can be considered to occur in two steps: Firstly, internal stresses are removed through heat treatment, and secondly, cooling is performed at such a rate as to prevent their return. Without this internal strain relief, changes in refractive index at different temperatures may have been misconstrued as a cross-sensitivity effect. In addition, Young's modulus for glass will be lower if there is residual strain present [16]. Both of these effects may introduce additional error into the measurements. Annealing not only removes mechanical strain, but also brings the glass to a condition approximating an internal equilibrium. Heat treatment, even below the annealing temperature, can result in a change in Young's modulus, with the value of Young's modulus increasing with decreasing annealing temperature. Morey [16] suggests that a period of 5 hours appears to be sufficient for most glasses to stabilize.

The linearity of the scan over the FSR of the FFP used in this work was investigated. The experimental arrangement comprised an APD that monitored the output from the FFP as it is scanned through a spectrum generated by a passive Fabry-Perot etalon. The rationale of the experiment was to analyse the linearity of the PZT displacement by monitoring a spectrum in which the constituent fringes had a constant optical frequency separation. Any deviation from a constant separation of the fringes would indicate a non-linearity in the PZT response, which could then be quantified. A passive FP etalon was formed between the ends of two fibres mounted on two separate translation stages; consequently, the cavity was adjusted easily to produce a spectrum with the desired fringe separation. The SLD was used to illuminate the etalon. The ramp waveform applied to the FFP and the resulting transmission spectrum were monitored simultaneously. The results showed a linearity within the manufacturers specifications (2 %) over the operational range used in the subsequent characterisation of the FBG strain response. All measurements were made relative to a temperature stabilised reference FBG spectrum. Slight modification of the finesse over the FSR arising from changes in the reflectivities of the dielectric films, over the full FSR was specified by the manufacturers to be less than two percent [17].

Another possible source of uncertainty was the method used to place the FBG under tensile strain. Although the PZT used to apply the strain was operated over its nominally linear region, it was important to avoid nonlinearity or hysteresis in the application of the strain. The FBG, on the other hand, is known to show no significant nonlinearity in wavelength shift as a function of applied strain, even if stretched up to breaking point [18]. To minimise the influence of these issues, the displacement of the stage was measured using a Michelson interferometer in which one reflector was mounted on the moveable stage. Any variation of the output of the interferometer from a perfect sinusoidal output could then be detected. As an additional precaution, the buffer coating was removed from the full length of fibre to be strained to eliminate any effect it might have on the FBG response

The Michelson interferometer employed a *Coherent 200* single frequency He-Ne laser. The laser was temperature stabilised to eliminate ambient temperature induced shifts in the emitted wavelength. The laser was specified to have a stability of $\leq \pm 1$ MHz per 5 minutes. The advantage of using the interferometer set-up was that linearisation of the applied strain was achieved in an absolute and independent fashion.

The resolution of the system was optimised by reducing the amplitude of the ramp applied to the FFP, such that the wavelength scan of the filter was limited to the maximum wavelength range expected for the level of applied strain. Thus, given the limited sampling frequency of the data acquisition card, the acquired spectrum contained the maximum possible number of samples. A scan frequency of 6.06 Hz was applied to the FFP, and the acquisition card sampled at 10^4 samples per second. The Bragg wavelengths were determined from the captured spectrum by fitting a quadratic polynomial to a group of consecutive data points and subsequently differentiating the fitted polynomial to determine if the group contained a maximum. The quadratic fit moved over the spectrum as a sliding window. The fitting routine interpolated between points. The overall resolution of the system, of 0.59 ± 0.04 pm, corresponding to 0.96 ± 0.07 $\mu\epsilon$, was achieved over 26 % of the FSR; consequently, this system provides a dynamic range of 45 dB. The

calibrated interrogation and demodulation scheme was then used to investigate the temperature effects on the strain response of a number of FBGs written into three different fibre types.

In order to predict the magnitude of change in response it was necessary to determine experimentally the thermal responses of the gratings. This was achieved by measuring the resonant wavelength of an FBG at a range of different temperatures, as shown in figure 3, for Fibrecore PS750. The sensitivity measured, $(7.0 \pm 0.2) \text{ pm} / ^\circ\text{C}$, is typical of the thermal sensitivity of FBGs.

The strain sensitivity was characterised at the highest temperature first. The temperature was subsequently decreased before the next set of readings. The measurements were performed in this fashion to ensure that any permanent thermal effect on the FBG resultant from the high temperature treatment would be the same for each subsequent temperature regime. The fibre was allowed to reach thermal equilibrium before any measurements were made. This was done to eliminate thermally induced stress due to temperature gradients through the fibre. This should be achieved for a 125 micron diameter fibre in about 30 seconds [19].

RESULTS AND DISCUSSION

The temperature dependence of the strain response was obtained for each of the fibres by measuring the strain response at a range of temperatures from 100°C to 400°C . The results for the Fibrecore fibre are shown in figures 4a-4e. Each data point is the average of 40 readings. The gradient of a straight line fitted through each of these sets of data points is then used to plot the strain response as a function of temperature. The results for this are shown for each fibre type in figures 5-7 and summarised in table 1. The gradient of a straight line fitted through these points then provides the thermal dependence of the strain response of each fibre type. These graphs show good linearity over the range of temperature used. The measurements show that there is a change in the response of the FBG at different temperatures, though the magnitude of this change is such that its effect would only be significant over large temperature or strain ranges ($\sim 0.5\%$ over a 1000°C). The experimental results indicate that the temperature dependence of the strain sensitivities of the

various fibre types investigated lie within the range $0.20 - 0.21 \text{ fm } \mu\epsilon^{-1} \text{ } ^\circ\text{C}^{-1}$, in agreement with the theoretical prediction of $0.2 \text{ fm } \mu\epsilon^{-1} \text{ } ^\circ\text{C}^{-1}$, within the bounds of the experimental errors quoted.

It is important to consider the influence of the experimental procedure upon the results. The variation in the temperature along the length of the tube furnace, $\pm 5 \text{ } ^\circ\text{C}$ over the central 4 cm, and the problem of ensuring that each FBG tested was at the same location in the furnace, complicates the comparison with the results obtained for the different fibres. However, for any given fibre, the location of the FBG within the furnace was maintained throughout the strain sensitivity characterisation ensuring self consistent results.

Another complication when applying a tensile load to the fibre at higher temperatures is an error introduced by the inelastic behaviour of the fibre, effectively further drawing the fibre. This will have the effect of changing the mechanical properties and the pitch of the FBGs. Further reason for not characterising the strain sensitivity at higher temperatures are cross-sensitivity effects which result in measurement errors that increase in proportion to the product of strain and temperature [20]. As a result, strain sensitivity characterisation performed at high temperatures will be inherently more erroneous than that performed at lower temperatures. The hysteresis effect previously observed for prolonged strain application at $650 \text{ } ^\circ\text{C}$ [5] was not observed in these experiments. This is probably a result of the lower temperatures employed, which avoid the transition range for silica fibre, where the application of a tensile load may result in the further drawing of the fibre.

A potential improvement in the measurement of the variation in the strain response with temperature might be to include a second reference in the oven to account for miscellaneous temperature effects. It is possible that thermal fluctuations could be misinterpreted as strain. This internal reference FBG would experience a similar thermal environment to the sensor under strain making it possible to separate out additional factors other than applied strain that affected the response of the sensor.

CONCLUSIONS

The temperature effects on the strain responses of in-fibre Bragg gratings (FBGs) written into three differing fibre types has been investigated. It was found that these responses changed on average by 0.21 ± 0.03 fm $\mu\epsilon^{-1} \text{ } ^\circ\text{C}^{-1}$ over a temperature range of 100-400 $^\circ\text{C}$. The results obtained are in agreement, to within the experimental error, with predictions based on material parameters.

ACKNOWLEDGMENTS

Martin O'Dwyer acknowledges the support of a European Commission Training and Mobility of Researchers (TMR) grant. The authors would like to thank Stephen Staines for his assistance with experimental aspects of this work.

References

- [1] A. Othonos and K. Kalli *Fibre Bragg gratings, Fundamentals and Applications in Telecommunications and Sensing* (London: Artech House Publishing). 1999.
- [2] K.O. Hill, Y. Fujii, D.C. Johnson, and B.S. Kawasaki, *Photosensitivity in optical fibre waveguides: Application to reflection filter fabrication*, Appl.Phys.Lett., **32**, pp. 647-649, 1978.
- [3] G.M.H. Flockhart, W.N. MacPherson, J.S. Barton, J.D.C. Jones, L. Zhang, I. Bennion, *Departure from linearity of fibre Bragg grating temperature coefficients*, OFS 2002: 15TH Optical Fibre Sensors Conference Technical Digest, pp75-78, 2002.
- [4] M. Ayub, R.C. Spooncer, and B.E. Jones, *Measurement of the temperature dependence of the stress-optic coefficient of photoelastic materials*, Proc. Institute of Physics, **111**, pp. 373-378, 1990.
- [5] W.W. Morey, G. Meltz, and J.M. Weiss., *High temperature capabilities and limitations of fiber grating sensors*, Proc. SPIE, **2360**, pp 234-237, 1994.
- [6] T. Baak, *Thermal coefficient of refractive index of optical glasses*, J.Opt.Soc.Am., **59**, pp. 851-857, 1969.
- [7] L. Prod'homme, *A new approach to the thermal change in the refractive index of glasses*, Physics and Chemistry of Glasses, **1**, pp. 119-122, 1960.
- [8] H. Scholze, *Glass; Nature, Structure, and Properties*, Springer-Verlag, New York, 1991.
- [9] A.J. Barlow and D.N Payne, *The stress optic effect in optical fibres*, IEEE J.Quantum Electron., **QE-19**, pp. 834-839, 1983.
- [10] J.S. Sirkis, *Unified approach to phase-strain-temperature models for smart structure interferometric optical fiber sensors: part 1, development*, Opt.Eng., **32**, pp 752-761, 1993.
- [11] A. Bertholds, R. Dandliker, *Determination of the individual strain-optic coefficients in single mode optical fibers*, J.Lightwave Technol., **6**, pp. 17-20, 1988.
- [12] A.D. Kersey, T.A. Berkoff, W.W. Morey, *Multiplexed fiber Bragg grating strain-sensor with a fiber Fabry-Perot filter*, Opt.Lett., **18**, pp. 1370-1371, 1993.

- [13] M.L. Dockney, S.W. James and R.P. Tatam, *Fibre Bragg gratings fabricated using a wavelength tuneable laser source and a phase mask based interferometer*, Meas.Sci.Technol., **7**, pp. 445-448, 1995.
- [14] B. Malo, J. Albert, K.O. Hill, F. Bilodeau, D.C. Johnson, *Effective index drift from molecular hydrogen diffusion in hydrogen-loaded optical fibres and its effect on Bragg grating fabrication*, Electron.Lett., **30**, pp. 442-443, 1994.
- [15] H.J. Patrick, S.L. Gilbert, A. Lidgard, M.D. Gallagher, *Annealing of Bragg gratings in hydrogen-loaded optical fiber*, J.Appl.Phys., **78**, pp.2940-2945, 1995.
- [16] G.W. Morey, *The properties of glass: 2nd edition*, Reinhold publishing corp., New York, 1954.
- [17] Micron Optics Inc, Private Communication.
- [18] N.Y. Ning, A. Meldrum, W.J. Shi, B.T. Meggitt , A.W. Palmer, K.T.V. Grattan and L. Li, *Bragg grating sensing instrument using a tuneable Fabry-Perot filter to detect wavelength variations*, Meas.Sci.Technol., **9**, pp. 599-606, 1998.
- [19] H. Rawson, *Properties and applications of glass*, Elsevier scientific publishing company, Amsterdam, Oxford, New York, 1980.
- [20] W. Jin, W.C. Michie, G. Thursby, M. Konstantaki, B. Culshaw, *Simultaneous measurement of strain and temperature: error analysis*, Opt.Eng., **36**, pp. 98-109, 1997.

Table 1. Measured temperature dependence of the strain sensitivity of the fibres studied in the temperature range 100-400 °C.

| Fibre Type | Temperature sensitivity ($\text{pm}^\circ\text{C}^{-1}$) | Temperature dependence of strain sensitivity ($\text{fm } \mu\epsilon^{-1} \text{ }^\circ\text{C}^{-1}$) |
|--|---|--|
| 3M 34LB3102 (80 μm diameter cladding) | 7.84 ± 0.04 | 0.20 ± 0.03 |
| Lightwave Technology FO808C | 7.7 ± 0.3 | 0.21 ± 0.03 |
| Fibrecore PS750 | 7.0 ± 0.2 | 0.21 ± 0.02 |

Figure Captions

Figure 1: Simulation of the temperature induced change in the strain response of an FBG with a Bragg wavelength of 850 nm. The temperature dependence of the strain sensitivity of FBG sensors is predicted to be $0.2 \text{ fm } \mu\epsilon^{-1} \text{ } ^\circ\text{C}^{-1}$.

Figure 2: A schematic of the experimental configuration. FFP – fibre Fabry Perot scanning filter, APD – Avalanche photodiode, SLD Super luminescent diode, CRO – oscilloscope.

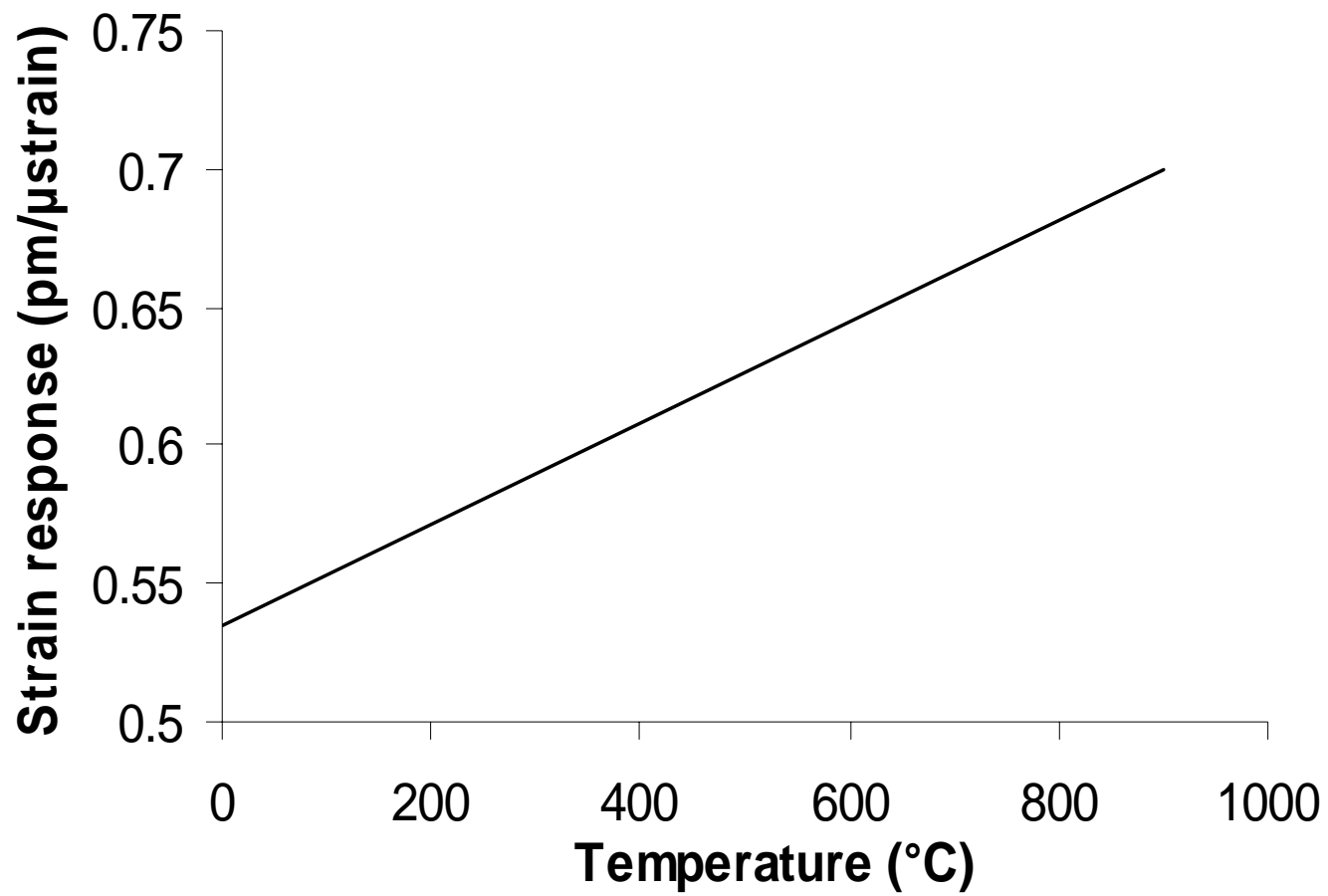
Figure 3: Temperature response of a FBG fabricated in PS750 Boron-Germania co-doped photosensitive optical fibre. The line is a linear regression fit to the data. The temperature sensitivity was found to be $7.0 \pm 0.2 \text{ pm } ^\circ\text{C}^{-1}$.

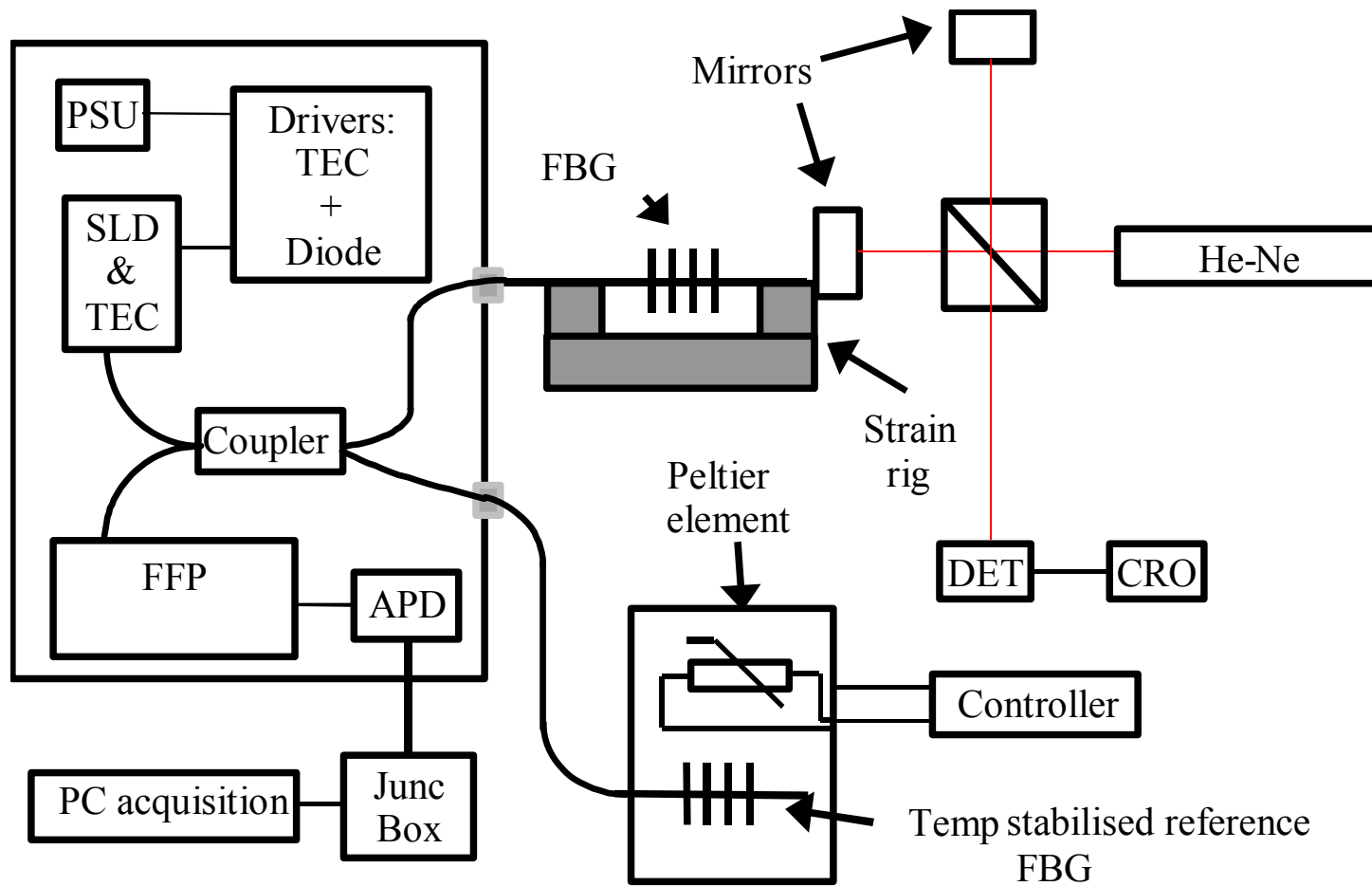
Figure 4: Strain response of Fibrecore PS750 Boron -Germania co-doped photosensitive optical fibre at a range of temperatures: a) 100°C , b) 175°C , c) 250°C , d) 325°C , e) 400°C . Each data point is the mean of 40 readings. The strain responses are: a) $(0.617 \pm 0.007) \text{ pm}/\mu\epsilon$; b) $(0.628 \pm 0.005) \text{ pm}/\mu\epsilon$; c) $(0.644 \pm 0.008) \text{ pm}/\mu\epsilon$; d) $(0.653 \pm 0.006) \text{ pm}/\mu\epsilon$; e) $(0.68 \pm 0.01) \text{ pm}/\mu\epsilon$.

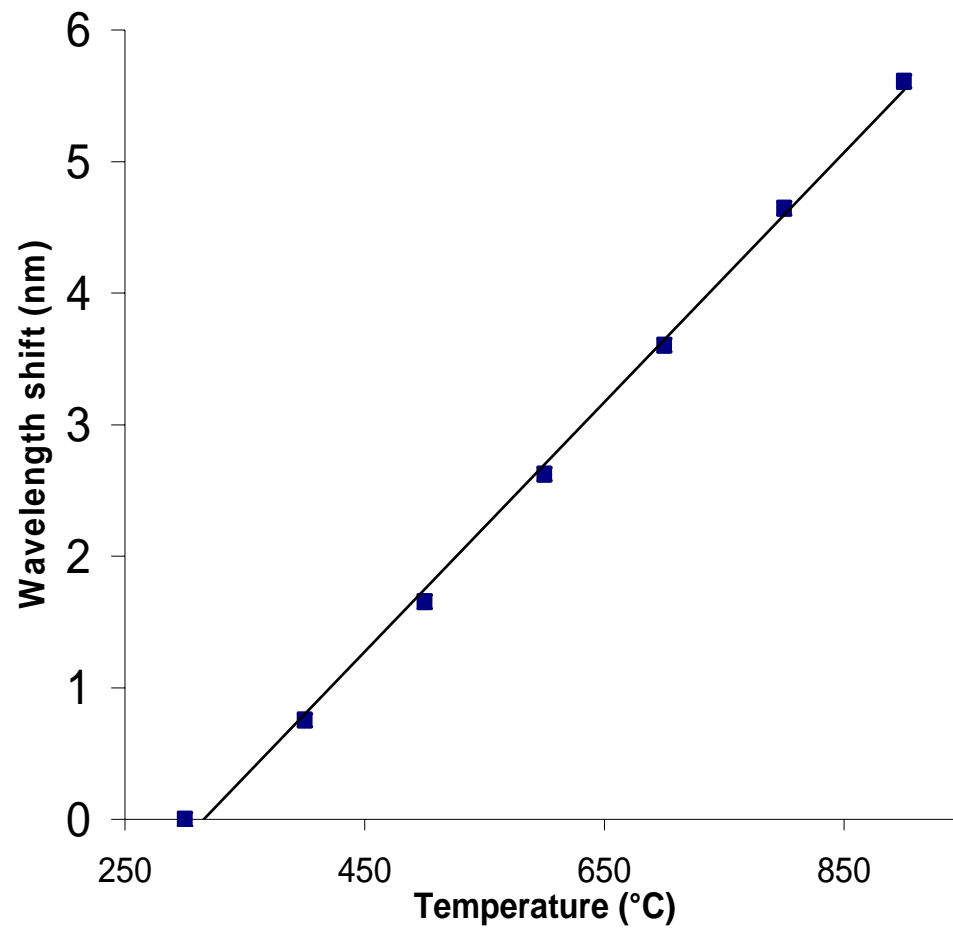
Figure 5: The strain sensitivity of Fibrecore PS750 Boron-Germania co-doped photosensitive optical fibre plotted as a function of temperature. The strain sensitivity was found to change by $0.21 \pm 0.02 \text{ fm } \mu\epsilon^{-1} \text{ } ^\circ\text{C}^{-1}$.

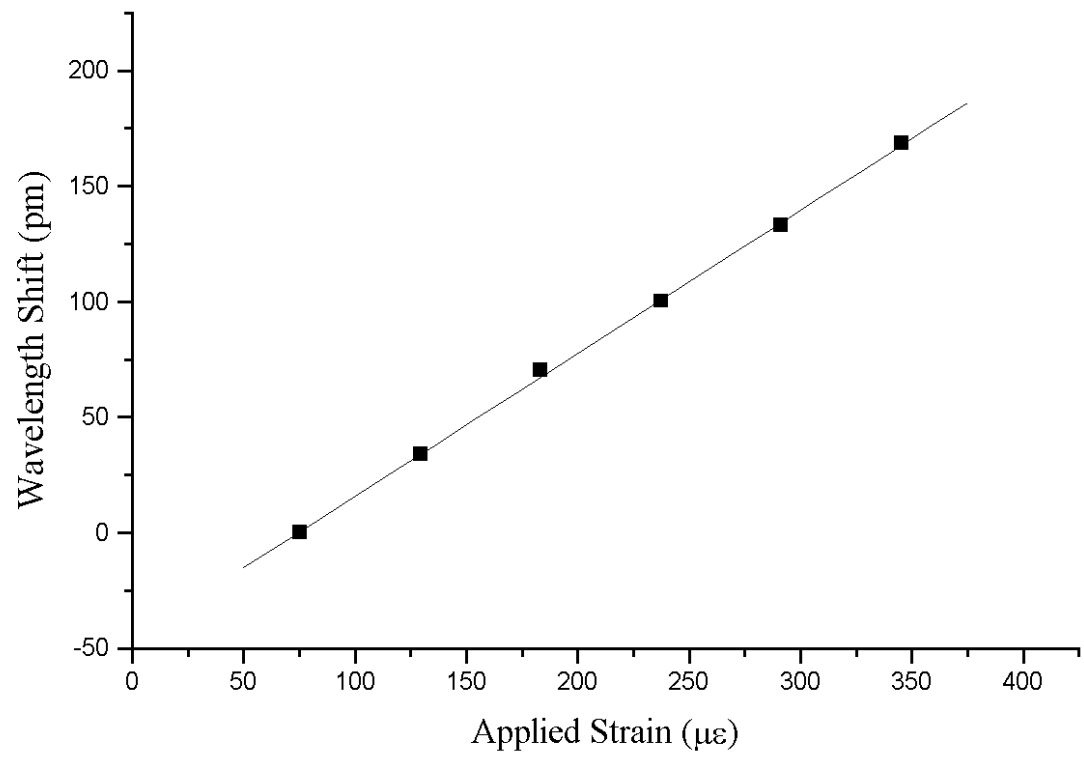
Figure 6: The strain sensitivity of Lightwave technology fibre, FO808C, plotted as a function of temperature. The strain sensitivity was found to change by $0.21 \pm 0.03 \text{ fm } \mu\epsilon^{-1} \text{ } ^\circ\text{C}^{-1}$.

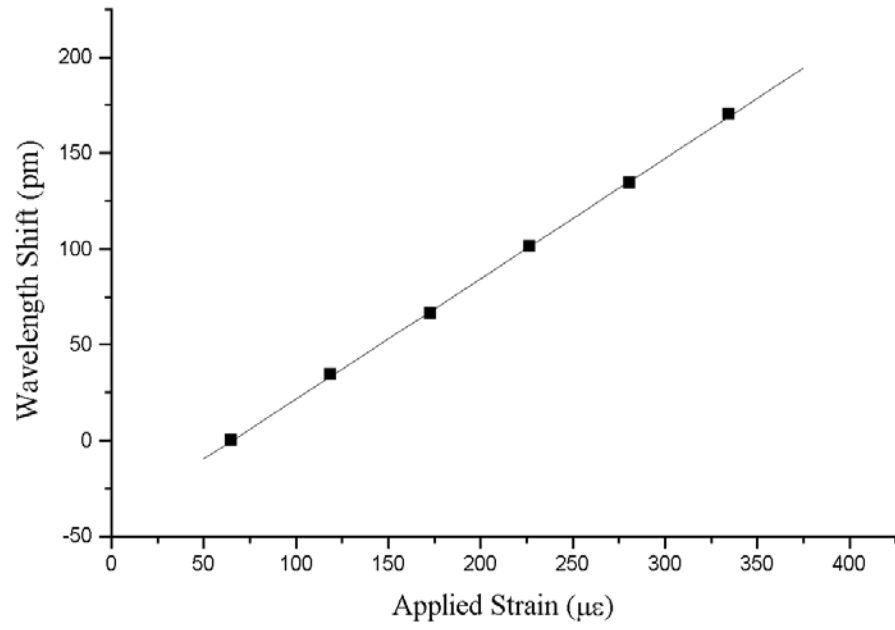
Figure 7: The strain sensitivity 3M 80 μ m cladding diameter optical fibre plotted as a function of temperature. The strain sensitivity was found to change by $0.20 \pm 0.03 \text{ fm } \mu\epsilon^{-1} \text{ } ^\circ\text{C}^{-1}$.

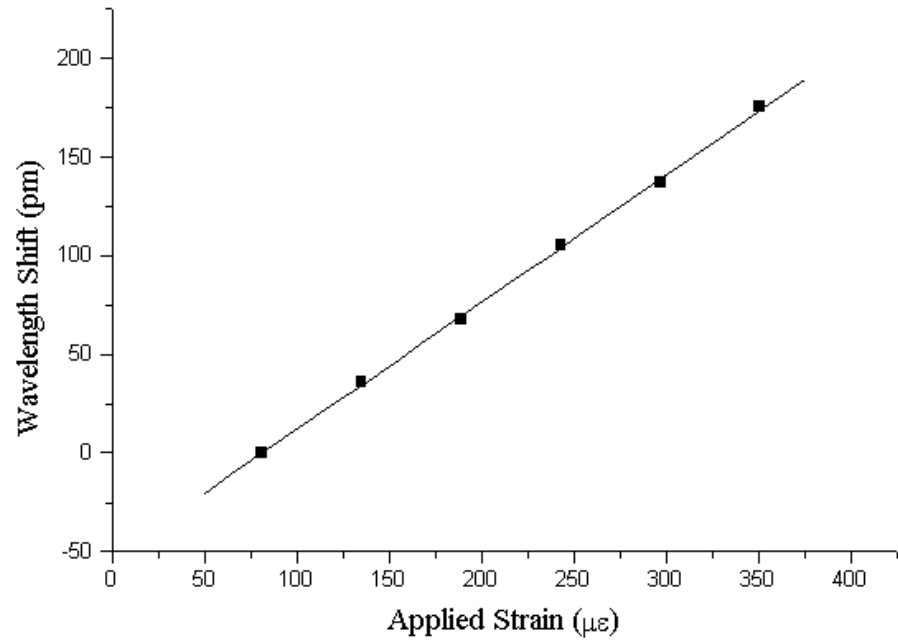


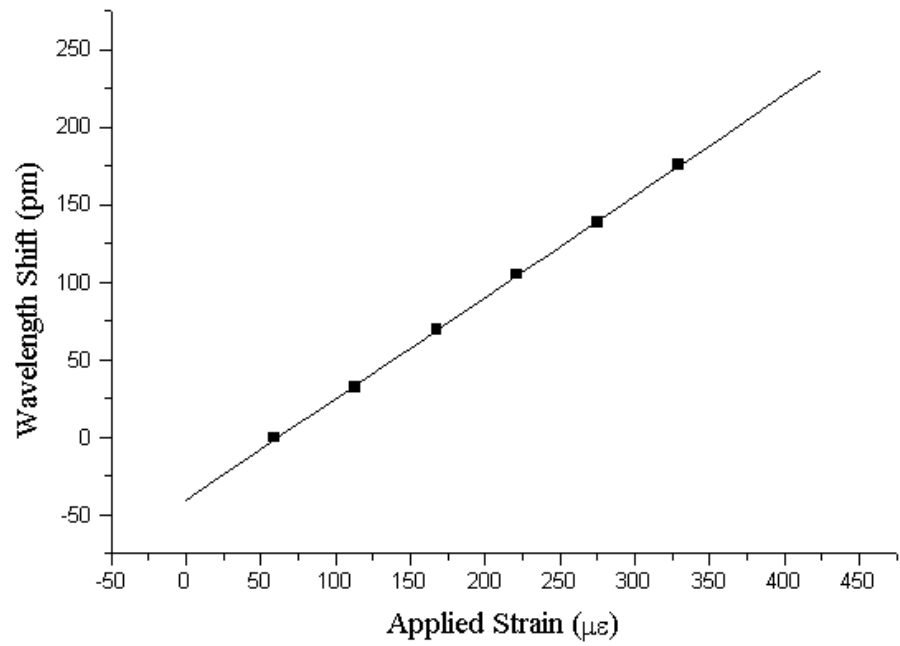


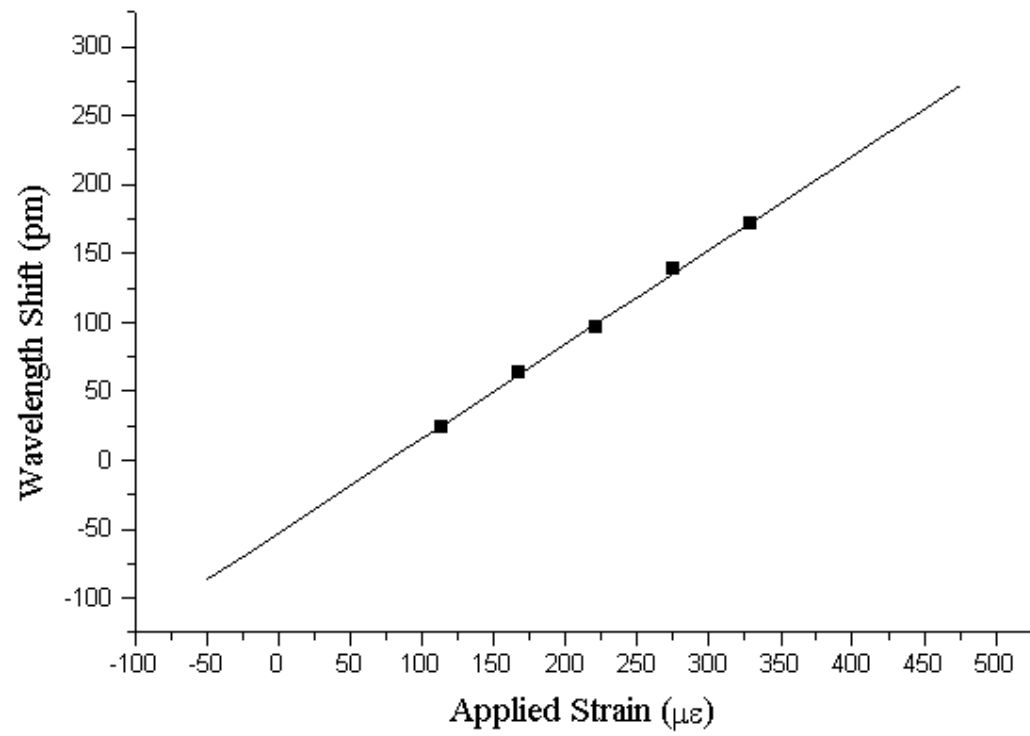


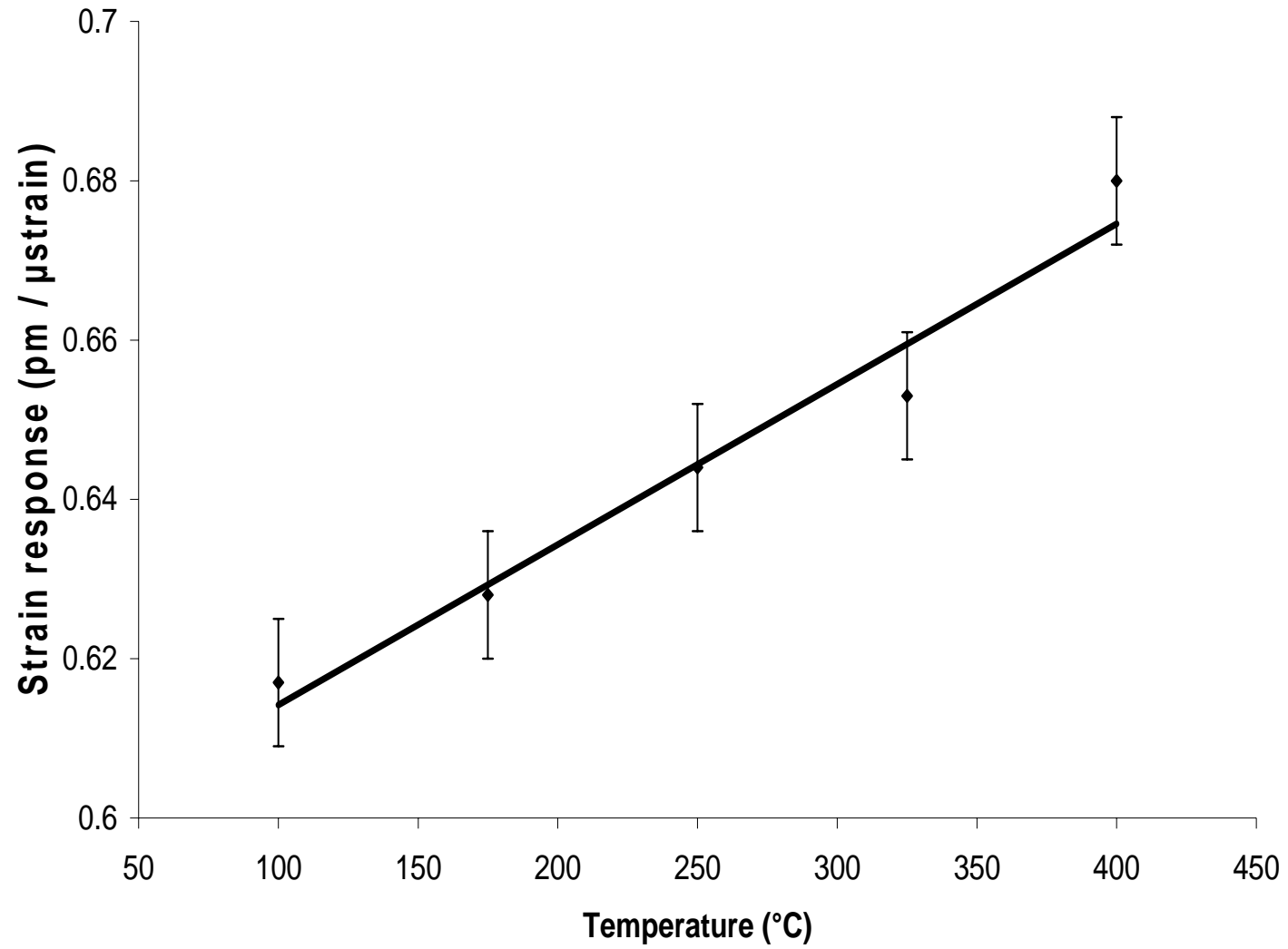


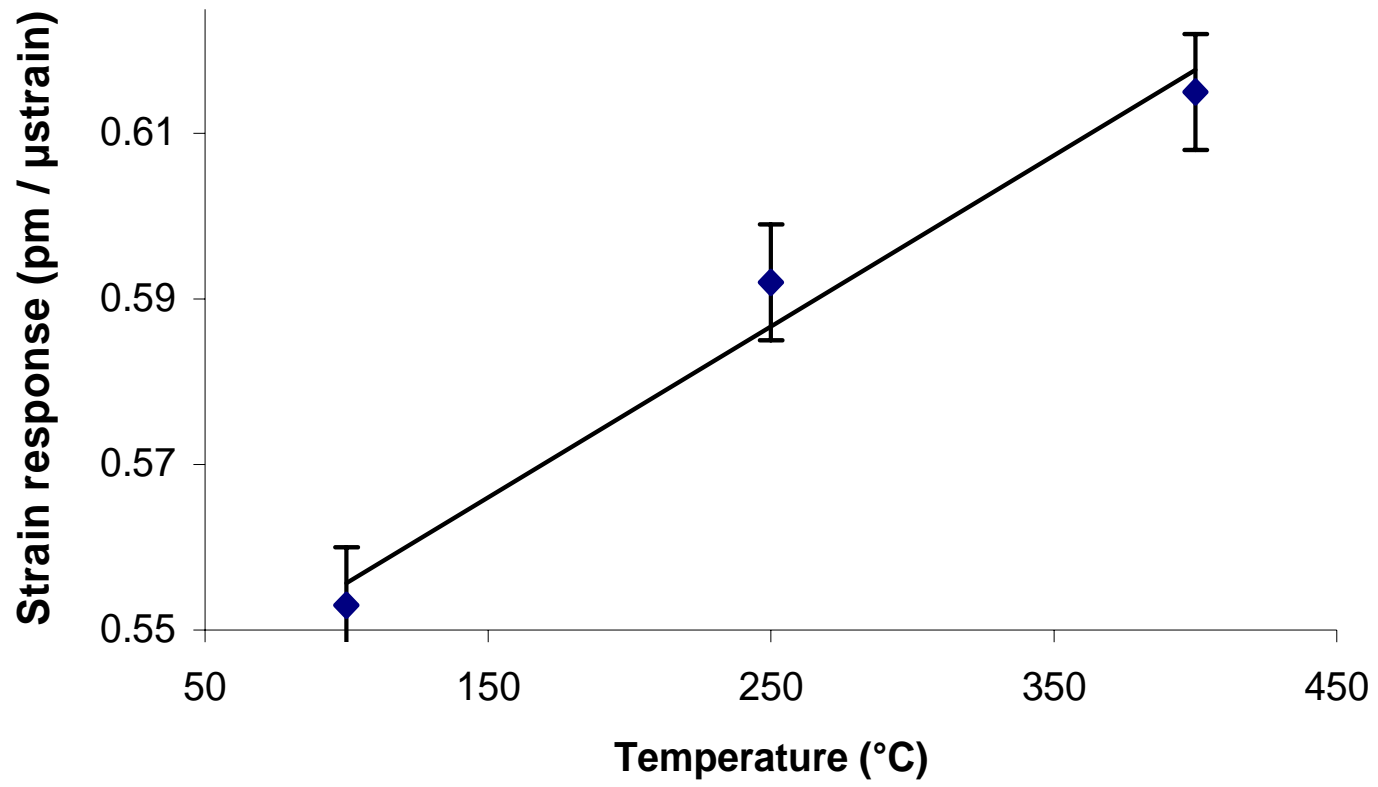


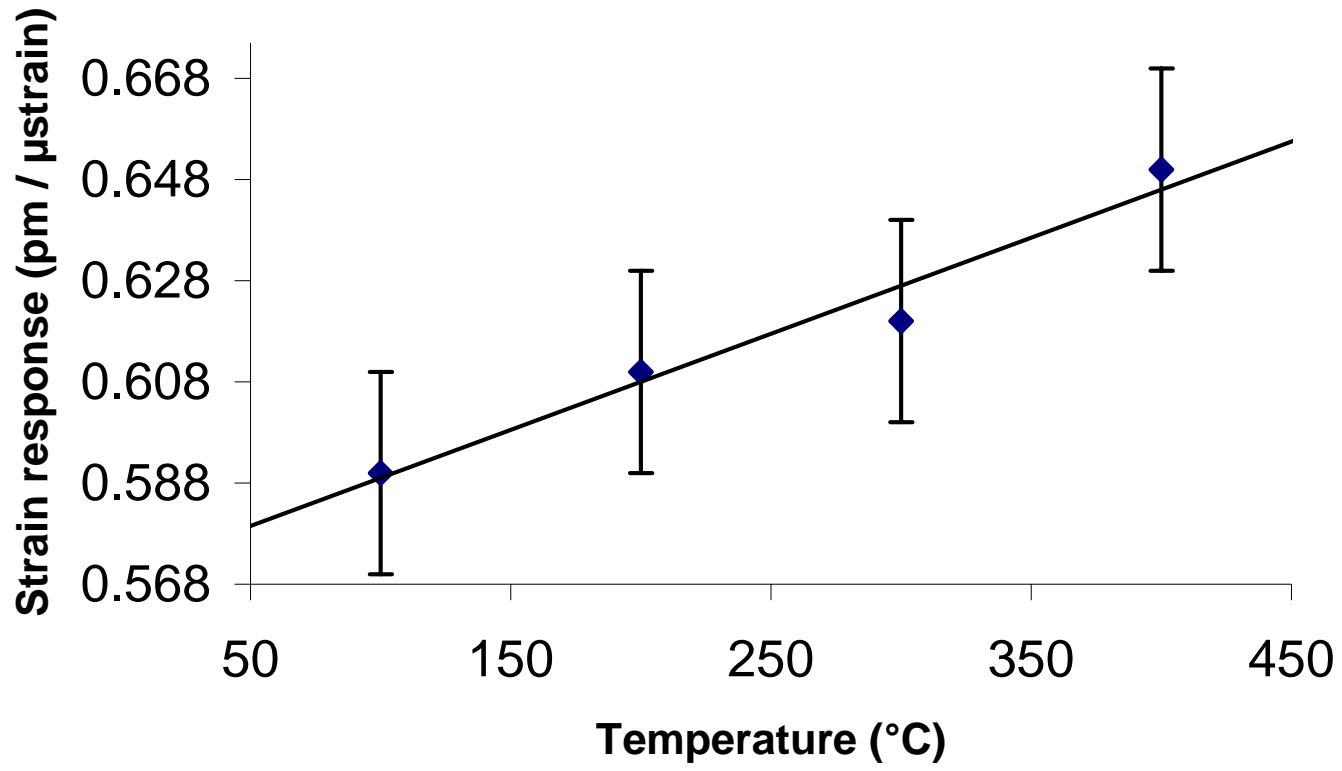












Thermal dependence of the strain response of optical fibre Bragg gratings.

O'Dwyer, Martin

2004-08-01T00:00:00Z

Martin J O'Dwyer, Chen-Chun Ye, Stephen W James and Ralph P Tatam; Thermal dependence of the strain response of optical fibre Bragg gratings, *Measurement Science and Technology*, Vol. 15, No. 8, Special Issue: Optical Fiber Sensors 16, August 2004, pp1607-1613

<http://dx.doi.org/10.1088/0957-0233/15/8/031>

Downloaded from CERES Research Repository, Cranfield University